Physics of laser plasma interaction in the context of shock ignition

O. Klimo[1], C. Riconda[2], S. Weber[3], J. Limpouch[1], X. Ribeyre[3], G. Schurtz[3], V. Tikhonchuk[3]

[1] *Czech Technical University in Prague, FNSPE, 11519, Prague, Czech Republic*

[2] *LULI, CNRS-CEA-Ecole Polytechnique-University Paris 6, 75252 Paris, France*

[3] *CELIA, University Bordeaux-CEA-CNRS, 33405 Talence, France*

In the Shock Ignition (SI) scheme the fuel assembly and ignition phases are separated. The ignition energy is supplied to the central hot spot by a strong converging shock launched by a high power laser spike with the intensity in the range of $10^{15} - 10^{16}$ W/cm^2 where nonlinear processes play an important role. We present here fully kinetic simulations covering the domain of transition from collisional- to collisionless-dominated laser absorption. The simulations were performed with a massively parallel relativistic electromagnetic PIC code in a 1D geometry. High order particle shapes, specially designed boundary conditions and relativistic Coulomb collisions included in the code.

The plasma parameters are defined in hydrodynamic simulations [1] relevant to the experiments [2]. They correspond to the time of the laser spike arrival, when the spherical target shell has already been accelerated and partially imploded. The corona electron temperature is $1.7 - 1.9$ keV, the ion temperature $0.5 - 1.1$ keV, the plasma Mach number is ranging from 1.5 to 3, the density profile is approximately exponential with the scale length of 400 μm. The simulation time was $50 - 100$ ps sufficient to achieve a quasi-stationary interaction regime. The laser pulse intensity is 1, 2.4 or 8 $\times 10^{15}$ W/cm^2 at the wavelength of 351 nm. The laser pulse has a 5 ps linear ramp at the beginning and than it stays on the maximum intensity. The ion charge is 3.5 and the ion mass is 7 times the proton mass (fully ionized deuteriated plastic CD). The collision frequency is calculated using a constant Coulomb logarithm, $\ln\Lambda = 10$. The linear gain analysis of the stimulated Brillouin (SBS) and Raman (SRS) scattering indicates that convective SBS amplification is very significant unless some other mechanism limits it. The SRS growth rate is strong in a small part of the density profile near the quarter critical density.

The temporal behavior of reflectivity and the temporally integrated spectrum of the reflected light at lower laser intensity 10^{15} W/cm^2 are presented in Fig. 1. Two runs – collisionless and with collisions included – are compared. The overall reflectivity in the collisionless case is more than 60%. The reflected light comes in a series of intense bunches that originate from the convectively amplified SBS waves. In the collisional case, the bunches of the reflected light are much less intense and the overall reflectivity is little less than 30%, which is expected from the linear theory of inverse bremsstrahlung absorption.

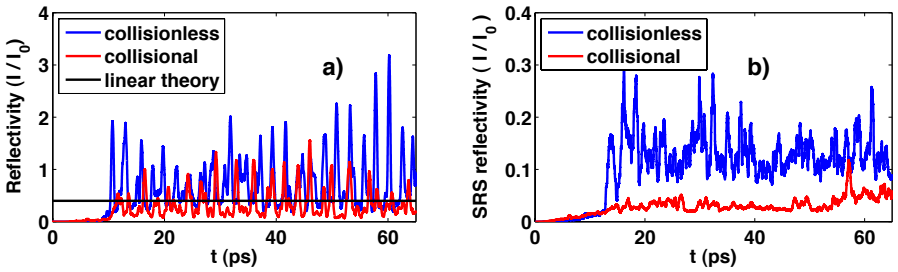

Figure 1: Temporal evolution of the reflectivity in the whole frequency range a) and in the frequency range corresponding to SRS ($\omega < 0.9\ \omega_0$) b) in the collisional and collisionless simulation of laser plasma interaction at the intensity 10^{15} W/cm^2. The expected value of the linear reflectivity $R = 40\%$ is included for comparison in panel a.

The reflectivity in the SRS frequency range ($\omega < 0.9\ \omega_0$) is below 5% level in the collisional simulation. This is in agreement with experimental measurements [2]. From the time of about 12 ps on, the reflected signal due to SRS is about 3 times stronger in the collisionless simulation. The time of 7 ps corresponds to 2 mm of light propagation, which is the distance from the front boundary of the simulation box to the quarter critical density.

The temporally resolved spectra of reflected light exhibit quantitative and qualitative differences between the collisional and collisionless cases. There are three distinct features in the frequency range from 0.5 ω_0 to ω_0: a narrow signal around ω_0 due to SBS, a broad spectrum around 0.7 ω_0 due to convective SRS and a strong signal around 0.5 ω_0 due to absolute SRS at quarter critical density. In the collisional case, the whole signal is weaker because of the lower reflectivity. In the collisionless case a strong signal at 0.25 ω_0 is observed. It comes from the secondary SRS process induced by the Raman scattered light at 1/16th of critical density [3].

The pulsating behavior of the SBS signal has been reported in many publications. It is explained by a strong convective gain of the scattered wave, which depletes completely the pump on its way out of plasma. The strength of the light pulse scattered by SBS is much weaker in the collisional case as the collisional damping of both, the incident and also the scattered light wave near the critical density is comparable to the SBS growth rate. Consequently, collisions play an important role in suppressing SBS instability in the low intensity case.

The energy distribution of electrons in the simulation box in the initial and final time (64 ps) are essentially Maxwellian with temperatures 2 keV and 2.5 keV, Fig. 2a. This clearly demonstrates efficient heating of the bulk population of electrons due to the collisional absorption process. Subtracting the initial energy distribution from the final one and integrating, we find the amount of absorbed energy, which is contained in thermal electrons. It is about 60% of the

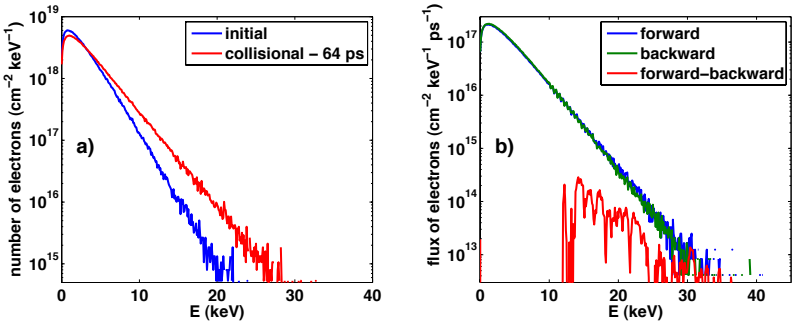

Figure 2: a) Electron energy distributions in the simulation box at the beginning (blue) and at the end (red) of the collisional simulation. b) Temporally averaged (over 64 ps) electron flux differential in energy pointing into in the target (forward-blue) and in the opposite direction (backward-green) recorded inside the target behind the quarter critical density. Subtraction of the forward and the backward flux (red) shows forward moving high energy electrons.

absorbed laser pulse energy, which is in agreement with the reflectivity data.

The energy transported by electrons was recorded at 40 μm behind the quarter critical density, Fig. 2b. Subtracting the backward (opposite to the laser propagation direction) flux from the forward one we obtain the distribution of higher energy electrons transporting the absorbed energy into the target. The distribution of these electrons extends from 10 to 30 keV. The energy transported by these higher energy electrons to about 20% of the absorbed laser pulse energy, that is, about 13% of the laser pulse energy. This is more than what can be produced by SRS (about 5%). The energy of these hot electrons is $4-12$ times higher than the bulk electron temperature. The collisional electron heating contributes to this hot electron population.

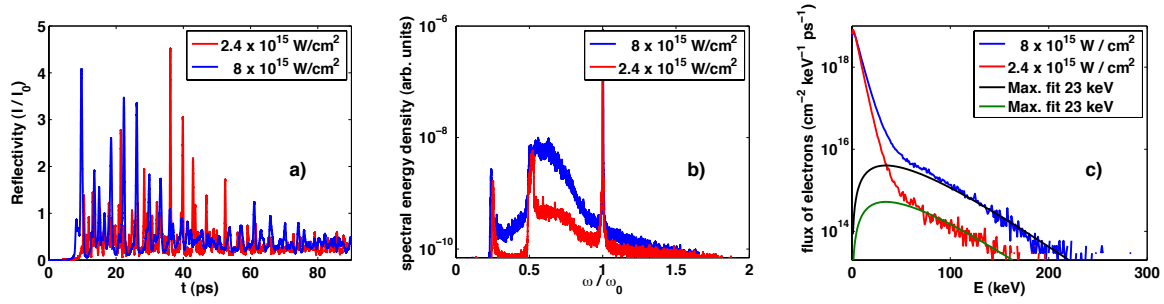

Figure 3: Temporal evolution of the reflectivity a) and temporally integrated spectrum of the reflected light b) in the simulations with the laser pulse intensity 2.4 and 8×10^{15} W/cm^2 (red and blue, respectively). c) Differential flux of electrons going in the dense plasma and the fits of the high energy tails with Maxwellian functions.

The importance of parametric processes increases at higher laser intensities. We demonstrate that by changing the laser pulse intensity to 2.4 and 8×10^{15} W/cm^2, while keeping the same initial temperature and density profiles. As it is shown in Fig. 3a, the reflectivity in both cases saturates at the level of about 35%. If the laser pulse is much longer than the transient stage taking $30 - 50$ ps, about 65% of its energy can absorbed in the target. For the higher intensity, this absorption is mostly due to a cascade of two SRS processes accompanied by the self-organized resonator between 1/4th and 1/16th of critical density [3].

The repartition between the collisional and collisionless processes in the spectra of reflected light, Fig. 3b, changes with the laser intensity. It follows from the energy distributions of electron that the fraction of energy absorbed by collisionless processes increases from 5 to 70 and 93% raising the laser pulse intensity from 1 to 2.4×10^{15} W/cm^2 and than to 8×10^{15} W/cm^2.

The differential (in energy) electron flux in Fig. 3c shows that the high energy tails correspond to the same temperature ~ 23 keV, while the number of hot electrons increases with the laser intensity. On the contrary, the temperature of thermal electrons increases with the laser intensity from 2.5 keV at the lowest intensity to 3 keV for the intensity 2.4×10^{15} W/cm^2 and to 4 keV at the maximum intensity. This temperature increase cannot be explained by collisional absorption, as the efficiency of this absorption mechanism significantly decreases (from about 60% to 20% and than to 5%) with increasing laser intensity.

In conclusion, in the lower end of the studied intensity range, the electron collisions largely suppress the SBS and about 70% of the laser pulse energy is absorbed. The SRS reflectivity remains at the level below 5%. At the upper boundary of the intensity domain, the collective effects dominate. The reflectivity remains at the level about 35% and the energy absorption occurs in the density cavities developing in the resonance zones near 1/4th and 1/16th of the critical density. The plasma reflectivities and the hot electrons are in a relatively good agreement with the results measured at the Omega laser [2]. The comparison with the measured spectra of SRS are less satisfactory, in particular, in what concerns the signal at the half-harmonic of the laser frequency. This problem deserves more studies.

This work is performed within the EU HiPER project and supported by EURATOM. The support of O.K. by the Czech Science Foundation, project P205/11/P660 is acknowledged.

References

[1] X. Ribeyre, *et al.*, Plasma Phys. Contr. Fusion, **51**, 015013 (2009).

[2] W. Theobald, *et al.*, Plasma Phys. Contr. Fusion, **51**, 124052 (2009).

[3] O. Klimo, *et al.*, Plasma Phys. Contr. Fusion, **52**, 055013 (2010).